



ELSEVIER

Available online at www.sciencedirect.com

SCIENCE @ DIRECT®

Physics of the Earth and Planetary Interiors 148 (2005) 131–148

PHYSICS
OF THE EARTH
AND PLANETARY
INTERIORS

www.elsevier.com/locate/pepi

Stochastic features of scattering

Tae-Kyung Hong^{a,*}, Ru-Shan Wu^a, B.L.N. Kennett^b

^a Earth Sciences Department/IGPP, University of California Santa Cruz, 1156 High Street, Santa Cruz, CA 95064, USA

^b Research School of Earth Sciences, The Australian National University, Canberra, ACT 0200, Australia

Received 11 March 2004; received in revised form 27 July 2004; accepted 6 August 2004

Abstract

The characteristics of scattering of scalar waves in stochastic random media are investigated in through the behaviour of the meanfield, scattering attenuation, and transmission fluctuations of amplitude and phase. Coherent scattered waves develop with increase of perturbation level, with the strength of the coherency varying with the type of media. The frequency content of the coherent scattered waves is close to that of the incident waves, and the phase is dependent on the statistical effect of the heterogeneities along the propagation path. The normalized scattering attenuation (Q_s^{-1}/ϵ^2) is stable at low normalized wavenumbers ($ka < 1$) regardless of the perturbation strength, but varies with the perturbation strength at high normalized wavenumbers ($ka > 1$). The coherent scattered waves, which strengthen with the perturbation level, add energy to the primary waves and reduce the apparent scattering attenuation. Stable measurements of normalized scattering attenuation can be made for sufficiently large distances. An empirical distance criterion for such stable measurements of scattering attenuation is presented in terms of propagation distance, incident wavelength, and the correlation length of the heterogeneities in the medium. The transmission fluctuation of amplitude and phase shows a high variation at large spatial lags, and the trend of the variation is dependent on the nature of heterogeneities. The ensemble average of amplitude fluctuation closely follows the theoretical prediction, but rather poor agreement is displayed for phase fluctuation. The effect of self-averaging during propagation in random media can not replace the ensemble averaging for mean transmission fluctuations of the amplitude and phase in random media.

© 2004 Elsevier B.V. All rights reserved.

Keywords: Stochastic effect; Scattering; Scalar waves; Scattering attenuation; Meanfield; Transmission fluctuation; Numerical modelling; Wavelet-based method; Wavelets

1. Introduction

The scattering of waves in heterogeneous media has been studied for many years in order to infer the physical properties of media (e.g., Nishimura et al., 2000; Line et al., 1998; Vidale and Earle, 2000) and to understand wave phenomena in the Earth (e.g., Aki and

* Corresponding author. Present address: Lamont-Doherty Earth Observatory of Columbia University, 61 Route 9W, Palisades, NY 10964, USA.

E-mail address: tkhong@ldeo.columbia.edu (T.-K. Hong).

Chouet, 1975; Wu and Aki, 1988; Sato and Fehler, 1998). In particular, analysis using coda waves allows the detection of a static (e.g., Korn, 1993; Nishimura et al., 2002) or a temporal velocity change in various regions (e.g., Ratdomopurbo and Poupinet, 1995; Nakahara et al., 1999; Snieder et al., 2002). However, most analysis based on primary waves requires information on the initial incident waves. Thus, field-data analyses based on primary waves can only be applied to those limited areas where information on the initial incident waves is available or can be replaced with other alternative information, for instance, the measurement of scattering attenuation (e.g., Yoshimoto et al., 2002) and inferences about the average physical properties from transmission fluctuation of amplitude and phase (e.g., Aki, 1973; Flatté and Wu, 1988; Line et al., 1998).

Some aspects of scattering (e.g., the variation of scattering attenuation) can be investigated under a controlled environment with the aid of numerical modelling (e.g., Frankel and Clayton, 1986; Roth and Korn, 1993). Despite some decades of studies, many aspects of scattering remain unclear. Although most analyses of scattering are based on some stochastic formulation, the features of stochastic scattering are not resolved clearly. Differences in the analysis procedures can lead to the magnitude of scattering attenuation varying by factor of two (Shapiro and Kneib, 1993). However, the investigation of physical factors influencing stochastic scattering has hardly been made.

Theoretical expressions based on a single backscattering approximation and forward scattering renormalization procedure (e.g., Wu, 1982b), are useful for the prediction of wave-related phenomena in weakly perturbed media. In particular, such theoretical curves of scattering attenuation are used as a reference for comparison with numerical results (Roth and Korn, 1993; Frankel and Clayton, 1986; Hong and Kennett, 2003a; Hong, 2004). In the formulation of theoretical scattering attenuation, the minimum scattering angle is a key parameter for the separation of forward scattered energy from backscattered energy that is responsible for the attenuation of the primary waves. There have been many studies to resolve the value of the minimum scattering angle via numerical modelling (e.g., Frankel and Clayton, 1986; Roth and Korn, 1993; Frenje and Juhlin, 2000; Hong and Kennett, 2003a) or theoretical approaches (Sato, 1982; Kawahara, 2002). However, it is still not clear whether the minimum scattering angle is

consistent or dependent on other parameters (e.g., perturbation strength, background velocity, etc.). Through studies on the variation of the minimum scattering angle as other parameters are changed, it will be possible to understand the effects of single and multiple scattering on attenuation.

Another observed phenomenon observed in waves transmitted through random media is fluctuation of amplitude and phase. After the development of theoretical expressions for the fluctuation rate of amplitude and phase in the transmitted waves (Chernov, 1960; Wu and Flatté, 1990; Shapiro and Kneib, 1993), there were efforts to identify the nature of media in terms of stochastic heterogeneities through comparison with these theoretical expressions (Aki, 1973; Capon, 1974; Line et al., 1998). However, Line et al. (1998) showed that the degree of agreement between theory and their synthetic data calculation varies significantly with the propagation distance. The applicability of the theoretical expressions to field data needs to be investigated.

Artificial attenuation can be raised in modelling for random media by the limitations of the accuracy of the numerical algorithm (Hong and Kennett, 2003a), and thus a highly accurate numerical modelling technique is demanded for the investigation. In this study, we apply a wavelet-based method (Hong and Kennett, 2002a,b), which retains high accuracy and stability even in modelling with strongly perturbed media.

2. Models and modeling technique

We consider the scattering of scalar waves in 2D random media. Scalar waves depend only on the velocity structure and correspond to acoustic waves in a medium with a constant density. The use of scalar waves simplifies the situation and concentrates attention on the influence of velocity perturbation on scattering. The influence of density perturbations has been investigated in a recent study (Hong et al., 2004). The scattering of elastic waves, which have wavetype coupling during scattering, was also studied in Hong and Kennett (2003a), Hong (2004). The features of scattering are expected to be similar between 2D and 3D problems although parameter estimates may be different (Frenje and Juhlin, 2000). 2D modelling simplifies the problems and saves much computational resources; we therefore investigate the features of scattering with

2D problems and infer the scattering features for 3D situations. The consideration of elastic waves requires the inclusions of the influence of energy partitioning by wavetype conversion, but the analysis procedure and the stochastic features are consistent with the scalar waves.

The domain employed has a size of 40 km \times 40 km which is represented by 512 \times 512 grid points. Plane waves are incident upward or downward and 128 receivers are placed along a line with a uniform spacing, 312.5 m. For the comparisons, various sets of physical parameters are considered, but the reference case has a background velocity of 2.5 km/s with a dominant frequency of the incident waves of 4.5 Hz. Artificial boundaries on both sides of the model are introduced with periodic boundary conditions, to simulate horizontally unbounded stochastic random media. The top and bottom boundaries of the domain are treated with absorbing boundary conditions. Random heterogeneities are constructed in the frequency domain by allocating random phases to the power spectral density function, and are added to the background homogeneous medium. (see, Roth and Korn, 1993).

Von Karman correlation functions are used for the construction of the stochastic random media. The autocorrelation function (ACF, $N(r, a)$) and the power spectral density function (PSDF, $\mathcal{P}(k, a)$) are given by

$$\begin{aligned} N(r, a) &= \frac{1}{2^{\nu-1}\Gamma(\nu)} \left(\frac{r}{a}\right)^{\nu} K_{\nu}\left(\frac{r}{a}\right), \\ \mathcal{P}(k, a) &= \frac{4\pi\nu a^2}{(1+k^2a^2)^{\nu+1}}, \end{aligned} \quad (1)$$

where r is the spatial lag, a the correlation distance, ν the Hurst number, Γ the Gamma function, k the wavenumber, and K_{ν} is the modified Bessel function of order ν . Note that the von Karman model with $\nu = 0.5$ corresponds to the exponential model.

A wavelet-based method (Hong and Kennett, 2002a,b, 2003a,b) is implemented for the simulation of wave propagation in random media. In this wavelet-based method, we recast the wave equations in the form of first-order differential equation system using a displacement–velocity formulation. The first-order differential equation system (i.e., a parabolic equation system in time) has an explicit discrete time solution with vector operators which are built from a set of spatial differential operators. These spatial differential operators

are represented through projection onto wavelet spaces. The various operations (e.g., spatial differentiations of wavefield) on the velocity and displacement wavefields are therefore made in wavelet domains. The implementation of spatial differentiation in a suite of wavelet spaces includes the influences of both high-frequency and low-frequency variation accurately, and so allows a high-accuracy numerical differentiation. In Hong and Kennett (2003a), it is shown that the wavelet-based method computes numerical differentiation accurately for a rapidly varying signal, while a fourth-order finite difference scheme generates artificially-attenuated results with a similar grid system. Moreover, the wavelet-based method is stable even in highly perturbed media with velocity variation of -96% to 96% , where normal grid-based methods suffer from severe numerical dispersion. We refer to Hong and Kennett (2002a,b, 2003a,b) for more details of the wavelet-based method.

3. Meanfields

For clarity, we distinguish between the meanfields in the time and spectral domains according to how the ensemble average (stacking) of wave responses is made. In this study, we employ an ‘uncorrected’ time meanfield without allowances for phase (or, travelttime) differences caused by heterogeneity in a medium. This time meanfield can be computed simply by stacking time responses. There is a tendency for an over-estimate of apparent attenuation in this case due to the interference between primary waves with different phases (Wu, 1982a; Sato and Fehler, 1998).

On the other hand, the spectral meanfield is calculated in Fourier domain by stacking the spectral amplitude of the primary waves. In order to reflect the pure effect of primary waves, only the primary wave portion is selected from each time response before Fourier transform by suppressing scattering wavefields (coda in this study) using a cosine bell time window (Kanasewich, 1981; Hong and Kennett, 2003a). Thus, unlike the time meanfield, the spectral meanfield is not affected by the travelttime differences. As a result, the consideration of the spectral meanfield allows better estimation of the scattering attenuation (Roth and Korn, 1993, see also, Section 4). Note that, however, time meanfields can be used efficiently for the investigation of scatterers deep in the Earth’s interior, where phase differences

are not expected to be significant (e.g., Hedlin et al., 1997).

A cosine-bell time window with an adaptive scale is used for selection of primary waves by considering the travel time fluctuation of transmitted waves through the random media. The travel time fluctuation increases with perturbation strength (ϵ), propagation distance (l), and the correlation length of heterogeneities (a). The cosine-bell window length for media with $c_0 = 2.5$ km/s, $f_d = 4.5$ Hz and $l = 29.1$ km, varies with the correlation length from $1.0T_p$ to $1.7T_p$. Here T_p is the duration time of primary waves in a homogeneous medium. The window length increases with the correlation length of heterogeneities since the phase fluctuation is proportional to the correlation length (see, Fig. 1(b)). Also, the tapering rate at the both sides of cosine bell varies with the window length of primary waves over the range $0.05T_p - 0.25T_p$. The magnitude of the travel time fluctuation varies with physical properties, so the window length is larger for a medium with a smaller c_0 or larger a , l , f_d . The scattered energy is distributed evenly with propagation dis-

tance due to self-averaging processes during propagation, thus the window time span is small enough that the level of scattered waves included in the time window is negligible compared to the primary energy. The broadening of the primary wave pulse in random media is discussed also in Sato (1989), Müller and Shapiro (2001).

A transmission fluctuation in amplitude and phase is developed by the local focusing and defocusing effects on the wavefield during propagation through heterogeneous regions (e.g., Hoshihara, 2000). Theoretically, the scattered waves generated by random heterogeneity are expected to be eliminated in the time meanfield by interference among the scattered waves with different (random) phases. However, as shown in Fig. 1, the coherent coda phases in the time meanfield increase with the perturbation strength. Note that the generation of coherent coda phase in scattered waves is observed also in laboratory experiments (Sivaji et al., 2002).

The magnitude of the mean coda varies with the type of media, but the wavetrains of the mean coda remain close between various media as long as the nature of heterogeneities (i.e., distribution of velocity

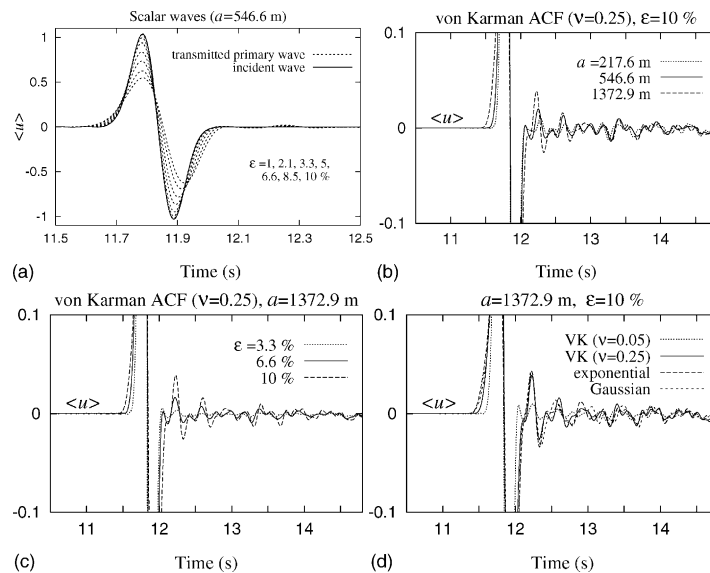


Fig. 1. (a) Variation of the time meanfield with changes of perturbation strength from 1% to 10%. The apparent attenuation in the time meanfield is increased due to the phase fluctuation in the time responses. The apparent attenuation increases with perturbation strength. Comparisons of magnified time meanfields for a change of (b) correlation distance, $a = 217.6, 546.6, 1372.9$ m, (c) perturbation strength, $\epsilon = 3.3\%, 6.6\%, 10\%$, and (d) the type of media (von Karman media, exponential, Gaussian). The magnitude of the mean coda increases with both the correlation length and the perturbation strength, but the phase and the wavetrain are nearly consistent for changes of correlation distance, perturbation strength and the type of medium.

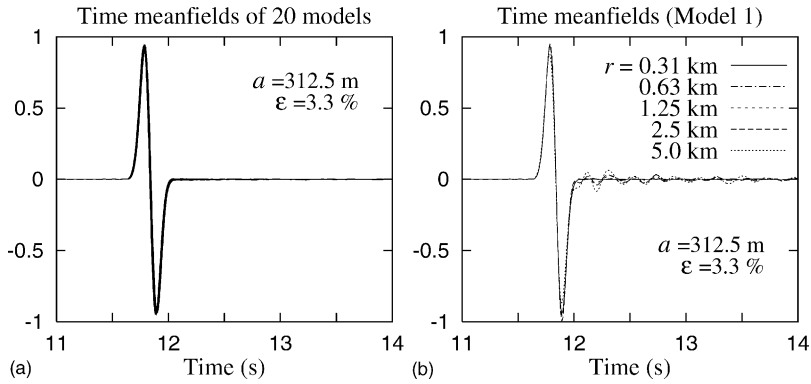


Fig. 2. (a) Comparison of time meanfields for 20 different realizations of the same stochastic model with $a = 312.5$ m and $\epsilon = 3.3\%$. The primary wave portions of the time meanfields are very similar to each other. (b) Variation of time meanfields for change of receiver spacing (r). The apparent mean coda increases with receiver spacing. A stable mean coda can be obtained for a dense array system.

perturbation) in the media is consistent. The frequency content of the mean coda is close to that of primary waves. Note also that the amplitude of apparent coherent phase increases with the spacing between receivers, but reaches a stable form when the receiver array is sufficiently dense (see, Fig. 2). The required receiver spacing depends on both the wavelength of primary waves (or, wavenumber k) and the correlation length of heterogeneity (a). The primary wave portions of time meanfields of 20 differently realizations of media with a low-perturbation level (3.3%), are very close to each other (Fig. 2(a)).

When, however, the distribution of heterogeneities in media is changed (i.e., differently styles of realization), the waveform of coherent scattered waves is

changed and the similarity does not exist (Fig. 3). That is, coherent scattered waves develop in random heterogeneous media and their amplitudes increase with the perturbation strength. Also, the phase of the coherent waves is a result of stochastic ensemble of propagation paths. Thus, as shown in Fig. 3, a change of the distribution order in heterogeneity, which is equivalent to a change of propagation direction (forward/backward), makes little difference. The interference of coherent scattered waves with primary waves appears to play an important role in the characteristics of the variation of scattering attenuation with perturbation strength (see, Section 4).

As a result of the interference between scattered waves and primary waves, the spectral meanfield dis-

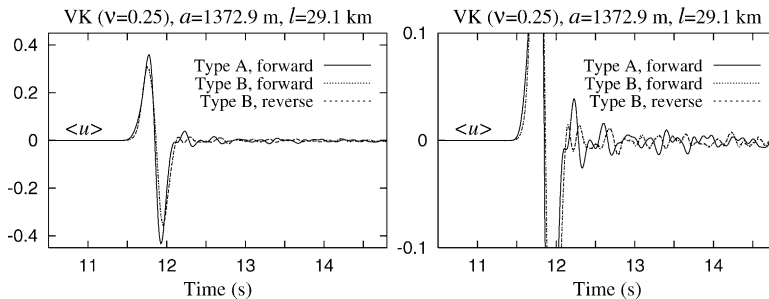


Fig. 3. Comparison of time meanfield for different media realizations. The right figure is a magnification of the left. The fluctuations of amplitude and phase in transmission are highly dependent on the nature of the heterogeneities encountered during propagation due to the different composite effects of focusing and defocusing on the wavefield. Not only the primary wave portion of the time meanfield, but also the coda wave portion displays a difference in amplitude and phase. The propagation direction does not makes any difference as long as the positions of the receivers and the source are reciprocal.

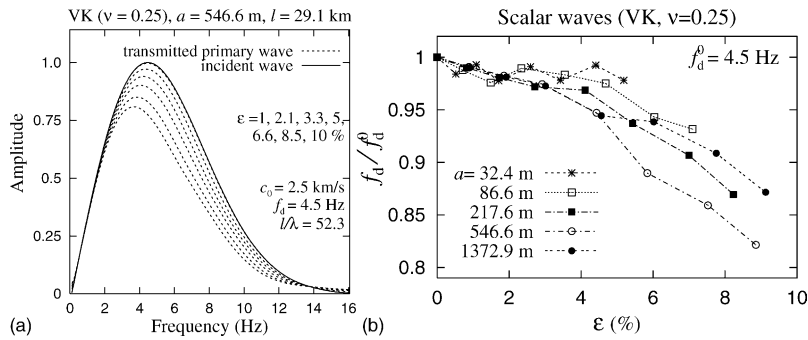


Fig. 4. (a) Apparent shift of dominant frequency of primary waves for a change of perturbation strength ($\epsilon = 1\%–10\%$) in a von Karman media with $\nu = 0.25$, correlation distance (a) 546.6 m, and background wavespeed (c_0) 2.5 km/s. The dominant frequency (f_d) of the plane incident waves is 4.5 Hz, and receivers are placed at a distance (l) of 29.1 km from the plane wave source position. The dominant frequency decreases with perturbation strength, but the low-frequency portion ($f < 2$ Hz) is barely affected by a change of perturbation strength. (b) The variation of apparent dominant frequency for a change of perturbation level in media with various correlation lengths ($a = 32.4–1372.9$ m). The rate of decrease differs above and below $\epsilon = 5\%$.

plays a characteristic apparent frequency shift from the initial situation, and this shift rate is proportional to the perturbation strength (Fig. 4). This apparent frequency shift develops mainly as a result of the nonuniform attenuation of energy with frequency. Note that frequency-dependence of the variation of seismic attenuation is a well-known feature (e.g., Yoshimoto et al., 2002). As shown in the figure, the strength of the frequency-dependent attenuation varies with the perturbation level. However, note that the low-frequency content ($f/f_d < 0.45$) is hardly attenuated even with high levels of perturbation (Fig. 4(a)). The features of attenuation are discussed in more detail in Section 4.

The estimates of the dominant frequencies for transmitted waves are close for media with various correlation lengths ($a = 32.4, 86.6, 217.6, 546.6, 1372.9$ m) when the perturbation level is low ($\leq 4\%$, see Fig. 4(b)). However, when the perturbation strength is larger than 6%, differentiated between the estimates of the dominant frequencies is obvious and varies with correlation distance. The largest shift of the dominant frequency occurs when the wavelength of incident waves is comparable to the scale of heterogeneities in media, i.e., at around $\lambda/a \sim 2$ in the figure.

The characteristic frequency shift looks important for application to geophysical inversion for seismic source time functions from field data (e.g., Singh et al., 2000). Seismic sources in tectonic regions usually occur in structures perturbed by tectonic activities, and seismic waves are influenced by the surrounding per-

turbed structures even in the initiation stage (Hong and Kennett, 2003b). Thus, with proper consideration of the loss of high-frequency information, it may be possible to recover a detailed source activation history, which otherwise can be underestimated due to energy transfer.

4. Scattering attenuation

4.1. Measurement and conditions

During propagation through a medium with random variation, primary waves are attenuated due to energy loss to scattering. The scattering attenuation of scalar (Wu, 1982b; Frenje and Juhlin, 2000), acoustic (Roth and Korn, 1993) and elastic waves (Frankel and Clayton, 1986; Hong and Kennett, 2003a) has been studied by using both theoretical estimates and numerical simulation techniques, and many aspects of scattering have been explored. In this section, we study factors that influence the scattering attenuation calculation and the way that attenuation changes.

First, in order to determine a stability criteria for estimates scattering attenuation (Q^{-1}) in terms of propagation distance, we consider various cases with different sets of background wave speeds and frequency content and compare the results. Twelve receiver arrays composed of 128 receivers with a uniform interval 312.5 m are deployed along the propagation direction with an

increment of 2.42 km from the plane wave source. The scattering attenuation rate is estimated using a spectral ratio technique ((Aki and Richards, 1980)):

$$Q_s^{-1} = \frac{2c_0}{\omega r} \ln \left[\frac{A_0(\omega)}{A_r(\omega)} \right], \quad (2)$$

where c_0 is the background wave speed, r the spatial lag (the propagation distance), ω the angular frequency of incident waves, and A_0 and A_r are the spectral amplitudes at the origin and at the receiver. The spectral amplitude of the primary waves is computed from a tapered time response which is designed to include mostly the primary wave portion (see, Section 3). The scattering attenuation is measured for a frequency band of 2–10 Hz around the dominant incident frequency (4.5 Hz). Note that the measurement of scattering attenuation using spectral amplitudes allows a accurate estimation, while measurements using time-record amplitudes may overestimate the scattering attenuation due to phase shifts and travel time anomalies (Roth and Korn, 1993).

Fig. 5 shows the variation of the scattering attenuation with changes of background velocity and frequency content. The theoretical expression of the scattering attenuation of 2D scalar waves (Q_s^{-1}) based on a single backscattering approximation, is given by (e.g., Wu, 1982b; Frankel and Clayton, 1986; Frenje and Juhlin, 2000)

$$\frac{Q_s^{-1}}{\epsilon^2} = \frac{k^2}{\pi} \int_{\theta_{\min}}^{\pi} \mathcal{P} \left(2k \sin \frac{\theta}{2}, a \right) d\theta, \quad (3)$$

where k is the wavenumber of incident waves, ϵ is the perturbation strength of medium, a is the correlation length of the heterogeneities, and ϵ is the perturbation strength of heterogeneities which corresponds to the standard deviation from the background property. Also, \mathcal{P} is a PSDF in (1), and θ_{\min} is the minimum scattering angle for exclusion of forward scattered energy from the scattering attenuation (see, Sato and Fehler, 1998). The theoretical scattering attenuation expression is developed from the idea that scattering energy loss is caused mainly by backscattering energy and forward scattering causes just a travel time anomaly in transmitted primary waves (Sato and Fehler, 1998). The minimum scattering angle is a reference angle for dividing between forward and backward scattering regimes in stochastic media. Various numer-

ical and theoretical studies have been made for the determination of the minimum scattering angle in various environments (e.g., Sato, 1982; Frankel and Clayton, 1986; Korn, 1993; Kawahara, 2002; Hong and Kennett, 2003a). Theoretically, the scattering attenuation in stochastic random media is expected to vary with normalized wavenumber (ka), the product of the incident wave wavenumber and the correlation length.

The measured scattering attenuation rates gradually approach to stable values with increase of propagation distance. The propagation distance required (l_c) for a stable measurement depends on the wavelength of incident waves and the correlation length of heterogeneities, and generally increases with the wavelength (λ) and the correlation length (a) (see, Fig. 5). In practice, l_c/λ increases with the correlation length of media, while $\log(l_c/a)$ decreases (see, Fig. 6), a linear regression estimate is

$$\left(\frac{l_c}{\lambda} \right) = -23.08 \log \left(\frac{l_c}{a} \right) + 76.01. \quad (4)$$

Thus, the condition of propagation distance (l) for stable measurement is

$$\left(\frac{l}{\lambda} \right) + 23.08 \log \left(\frac{l}{a} \right) - 76.01 > 0. \quad (5)$$

It is noteworthy that the magnitudes of the scattering attenuations varies slightly with the ratio of wavelength to correlation length (λ/a). The introduction of lower background wave velocity or higher frequency waves means that the high-frequency portion of incident waves is more attenuated. The magnitude of scattering attenuation varies also with the level of perturbation (Fig. 7). The normalized scattering attenuation rates (Q_s^{-1}/ϵ^2) decrease with perturbation strength at large normalized wavenumbers ($ka > 1$). These differences increases drastically with large ka , while the effect is hardly noticeable in the low normalized wavenumber regime. The magnitude of the scattering attenuation and its corresponding minimum scattering angle agrees with that from previous studies that considered weak perturbation levels (e.g., Roth and Korn, 1993). The large fluctuations in the measured scattering attenuation rates for $\epsilon = 1\%$ and $\lambda/a = 12.5$ results from numerical errors in the numerical analysis, e.g., the interpolation procedures for the computation of amplitude ratio as a function of frequency ($A_0(\omega)/A_r(\omega)$).

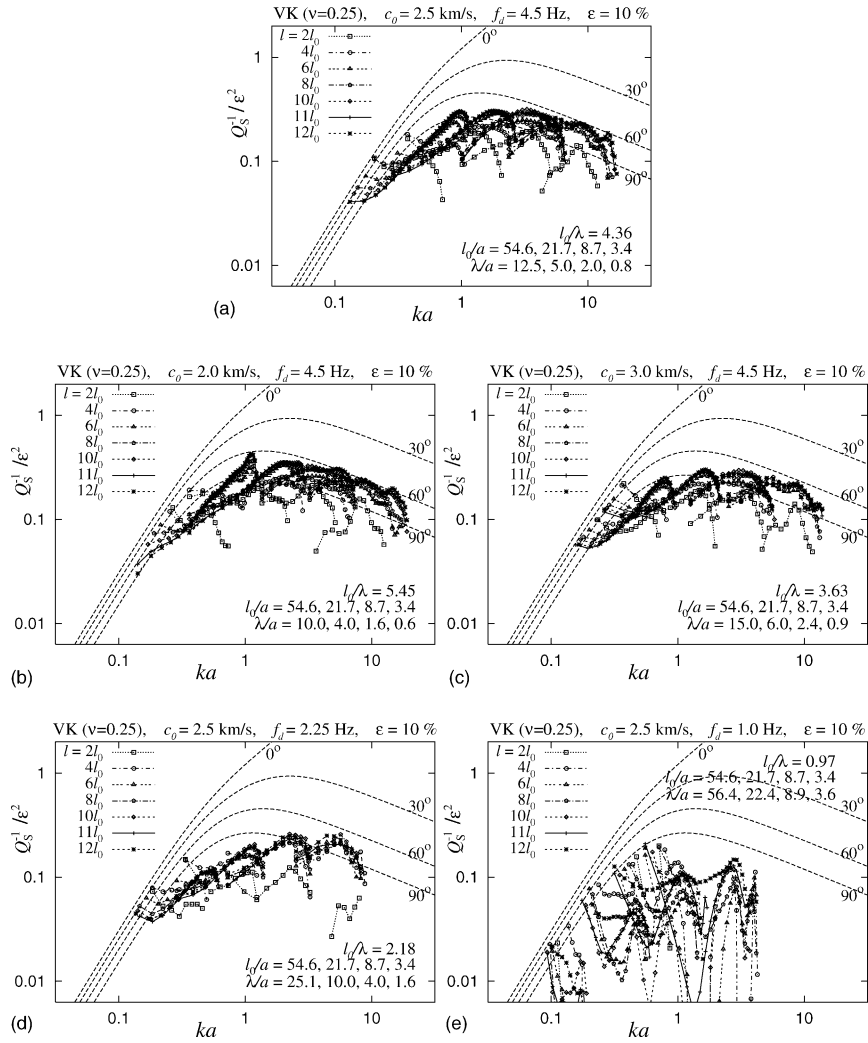


Fig. 5. Scattering attenuation variation with a change of propagation distance ($l = 2l_0 - 12l_0$, where $l_0 = 2.42$ km) for von Karman media ($\nu = 0.25$, $\epsilon = 10\%$) with various sets of background wavespeed (c_0) and dominant frequency of incident waves (f_d): (a) $c_0 = 2.5$ km/s, $f_d = 4.5$ Hz, (b) $c_0 = 2.0$ km/s, $f_d = 4.5$ Hz, (c) $c_0 = 3.0$ km/s, $f_d = 4.5$ Hz, (d) $c_0 = 2.5$ km/s, $f_d = 2.25$ Hz, (e) $c_0 = 2.5$ km/s, $f_d = 1.0$ Hz. The magnitude of scattering attenuation approaches a stable value with increase of propagation distance. The critical distance required for a stable measurement varies with the physical parameters of the medium. The required distance increases with both the correlation length of heterogeneities and the wavelength of incident waves.

4.2. Features

In Fig. 7, scattering attenuation is measured to be strongest at around $ka = 1$ corresponding to the theoretical prediction based on the single-back scattering approximation. This result is supported by various numerical studies for mildly perturbed (6.5%–10%) random media (e.g., Frankel and Clayton, 1986; Roth and Korn, 1993; Hong and Kennett, 2003a). The Fresnel

radius, within which constructive interference of ray reflection and mode conversion is expected, increases with the scale of heterogeneities (Flatté et al., 1979) and thus the effect of forward scattering effect is expected to be strong in a medium with large scales of heterogeneities. Thus, the measured scattering attenuation in the large ka regime is expected to be lower than that of the theoretical prediction from (3). However, the scattering attenuations from numerical experiments with

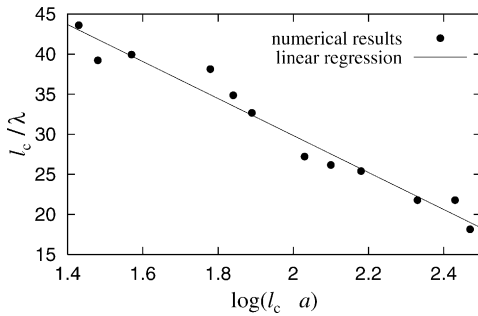


Fig. 6. The variation of the critical value of the dimensionless propagation distance (l_c/λ , $\log(l_c/a)$) for a stable measurement of the scattering attenuation Q_s^{-1} in terms of the correlation length and the wavelength. The linear regression result is represented by a solid line.

low-perturbation strengths ($\epsilon < 3.3\%$), which are expected to conform with the theoretical prediction based on the single backscattering approximation, actually increase with ka . This is because the first-order scattered waves interfere with adjacent heterogeneity to the propagation path, and a substantial portion of the first-order scattered waves is in fact scattered from the next heterogeneity as multi-scattered phases. This discrepancy between the current theory and numerical experiments needs further theoretical investigation.

The numerical results for a given band of frequency show that the variation of scattering attenuation with frequency depends on the scale of heterogeneity (a). For a medium with small heterogeneities ($ka \ll 1$), scattering attenuation increases with frequency, and vice versa for a medium with large heterogeneities ($ka \gg 1$). When, however, the wavelength of incident waves is comparable to the scale of heterogeneities ($ka \sim 1$), the scattering attenuation is observed to decrease with both increasing and decreasing frequency. This characteristic dependency of scattering attenuation on wave frequency and heterogeneity scales agrees with field observation (e.g., Tselentis, 1998).

Another eccentric pattern found in the numerical results is the decrease of normalized scattering attenuation (Q^{-1}/ϵ^2) with perturbation strength (ϵ) at large ka , unlike the theoretical prediction. The effect of multiscattering, in general, is anticipated to increase with perturbation strength. Thus, it might be expected to see more attenuation with increase of the perturbation strength at a heterogeneous medium. This discordant feature seems to result from an effect of stochastic scattering, the development of coherent scattered waves with increasing perturbation level, as discussed in Section 3. The coherent scattered waves increase with perturbation level and correlation length, and supplement the primary waves. Another possible source of the supplementary energy is forward scattered waves with a large scattering angle, $30^\circ < \theta < 90^\circ$. Single scattered waves with a large scattering angle are normally negligible for media with a weak perturbation level due to geometrical spreading and interference

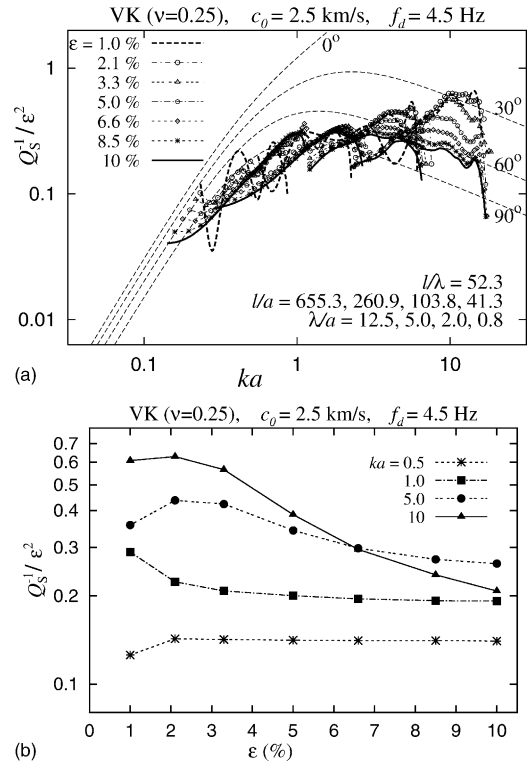


Fig. 7. (a) Variation of normalized scattering attenuation (Q_s^{-1}/ϵ^2) with a change of perturbation strength ($\epsilon = 1\%–10\%$). (b) Variation of scattering attenuation with perturbation strength at four representative normalized wavenumbers ($ka = 0.5, 1, 5, 10$). The scattering attenuation is measured at a distance of $l = 29.1$ km where stable measurement is expected from the empirical condition in (4). Scattering attenuation is proportional to the square of perturbation strength (ϵ^2) at a small ka ($ka < 1$), as expected in the theory. On the other hand, at a large ka ($ka > 1$), coherent scattered waves increase with perturbation level, and the normalized scattering attenuation for high-perturbation strength is observed to be less than that for low-perturbation strength. The discrepancy between normalized scattering attenuation for a change of perturbation strength increases with ka .

tic scattering, the development of coherent scattered waves with increasing perturbation level, as discussed in Section 3. The coherent scattered waves increase with perturbation level and correlation length, and supplement the primary waves. Another possible source of the supplementary energy is forward scattered waves with a large scattering angle, $30^\circ < \theta < 90^\circ$. Single scattered waves with a large scattering angle are normally negligible for media with a weak perturbation level due to geometrical spreading and interference

with other scattered phases. However, the single scattered waves become large in highly perturbed media and influence the later portion of the primary waves.

The scattering of waves redistributes a part of the incident energy, but the total physical energy is conserved inside the domain. The presence of intrinsic attenuation causes alteration of physical energy into chemical energy (e.g., heat), so the energy loss in the primary waves is hardly reflected in the coda energy. Moreover, the intrinsic energy absorption causes energy dissipation in the coda. Thus, a technique based on coda attenuation rates and coda envelopes was developed to separate of scattering and intrinsic attenuations (Wennerberg, 1993; Del Pezzo et al., 1995). However, attenuation rate of the coda can be changed with density perturbation strength (Hong et al., 2004). Thus, information on the relative variation of the density distribution required for a correct measurement. For detailed description of the measurement of scattering and intrinsic attenuations, we refer to studies with field data analysis (Ugalde et al., 1998; Hoshiya et al., 2001; Giampiccolo et al., 2004).

Scattering attenuation rate changes with the value of normalized wavenumber (ka) in a stochastic random medium where physical properties vary continuously, and the influence of a change in wavenumber (k) is nearly equivalent to a change in heterogeneity scale (a). However, in a recent study (Hong and Kennett, 2004), scattering attenuation in a medium with discretely distributed heterogeneities, which exhibit high impedance to background properties, shows a different dependence on the change in wavenumber and heterogeneity scale. For these discrete scatterers, when the incident wavenumber (frequency content) is changed with constant heterogeneity scale, the scattering attenuation displays a similar variation pattern with ka to the pattern for a stochastic random medium (i.e., increase and then decrease with ka), in agreement with theoretical studies of Kaelin and Johnson (1998a,b). In this situation, scattering attenuation increases with ka and remains constant for higher ka . However, when the incident frequency is changed and the heterogeneity is constant, the scattering attenuation decreases with ka after a critical value of ka . This pattern is close to the theoretical scattering attenuation variation expected in stochastic random media (Fig. 5). Therefore, when field data are analyzed, it may be necessary to consider the influence of both continuously varying heterogeneity

and discrete heterogeneities. For more details on the influence of discrete heterogeneities on scattering we refer to Hong and Kennett (2004).

We now measure the strength of waveform fluctuation (D_t) in order to see the influence of strong scattering on coherent scattered waves with a small scattering angle and incoherent scattered phases with a large scattering angle. We construct

$$D_t = \sqrt{\frac{1}{N_s} \sum_{j=1}^{N_s} (u_j - \langle u \rangle)^2}, \quad (6)$$

where u_j is the time response at the j th receiver, N_s is the number of receivers, and $\langle u \rangle$ is the time meanfield of records (see, Section 3). Mathematically, D_t corresponds to the standard deviation of the waveforms. The analysis allows us to understand the distribution and temporal variation of scattered energy. The magnitudes of D_t^2 for the coda corresponds to the intensity (energy) of back-scattered waves, and those in the primary wave portion indicate the strength of the amplitude and phase fluctuation of primary waves caused by scattered waves at small angles of deviation.

As shown in Fig. 8, the normalized intensity ($(D_t/\epsilon)^2$) in the late coda is nearly constant for various perturbation strengths. On the other hand, the normalized energy fluctuation for the primary wave portion decreases with perturbation level, and lasts for a couple of seconds in the early portion of the coda. From the variation of D_t/ϵ , multiple forward scattering appears to influence the whole range of primary waves and strong small angle scattered waves have an influence from the late portion of the primary waves through to the early portion of coda waves. In addition, the stable energy-level formation at late coda supports the idea of Aki and Chouet (1975) for a stable measurement of heterogeneity strength from late coda levels.

5. Transmission fluctuation of amplitude and phase

5.1. Theoretical expressions

There have been attempts to use the ratio of amplitude and phase fluctuations and their cross-correlations

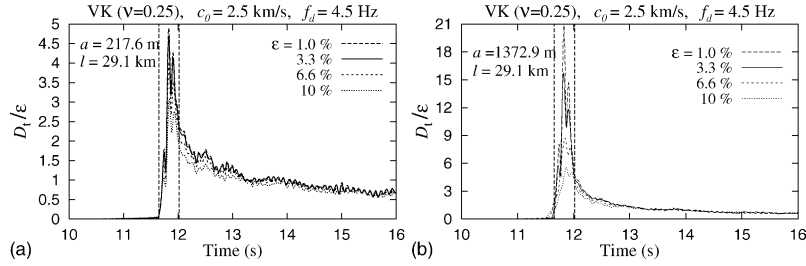


Fig. 8. Normalized wave-amplitude variance from the time meanfield for different perturbation strengths ($\epsilon = 1.0\%$, 3.3% , 6.6% , 10%) at von Karman media ($\nu = 0.25$) with correlation length $a = 217.6$ and 1372.9 m. The variance of the wave amplitude corresponds to the intensity (energy) of wavefield. The normalized energy for the late coda varies little for various perturbation strengths, but the intensity of the primary wave portion and the early coda depends on the perturbation strength. The discrepancy in the early coda supports the idea that coherent scattered waves develop with an increase of perturbation strength. The vertical broken lines indicate the time span of primary waves in a homogeneous medium (see, Fig. 1(a)).

to infer the physical parameters of media in terms of the characteristics of stochastic heterogeneity, such as the correlation length (Aki, 1973; Capon, 1974), through comparisons with theoretical predictions for Gaussian random media (Chernov, 1960). Substantial effort was made to develop an elegant technique based on information in the transmission fluctuations of amplitude and phase (Flatté and Wu, 1988; Wu and Flatté, 1990; Shapiro et al., 1996). However, the theoretical predictions, have rarely been examined for applicability to field data (Line et al., 1998).

The theoretical transmission fluctuations (auto- and cross-covariance) of the logarithmic amplitude (u) and phase (ϕ) are given by (Wu and Flatté, 1990; Line et al., 1998)

$$\begin{aligned} \langle u_1 u_2 \rangle(d) &= 2\pi k^2 \int_0^l dz \int_0^\infty \sin^2\left(\frac{\xi^2 z}{2k}\right) \cos(\xi d) \mathcal{P}_z(\xi, 0, z) d\xi, \\ \langle \phi_1 \phi_2 \rangle(d) &= 2\pi k^2 \int_0^l dz \int_0^\infty \cos^2\left(\frac{\xi^2 z}{2k}\right) \cos(\xi d) \mathcal{P}_z(\xi, 0, z) d\xi, \\ \langle u_1 \phi_2 \rangle(d) &= 2\pi k^2 \int_0^l dz \int_0^\infty \cos\left(\frac{\xi^2 z}{2k}\right) \sin\left(\frac{\xi^2 z}{2k}\right) \cos(\xi d) \mathcal{P}_z(\xi, 0, z) d\xi, \end{aligned} \quad (7)$$

where l is the propagation distance, d the spatial lag (the distance between the two receivers), and \mathcal{P}_z is the depth(z)-dependent power spectral density function (cf., (1)). Shapiro et al. (1996) formulated theoretical expressions for depth-independent auto-correlation functions with a similar approach, and they are equivalent to a simplified form of (7). The auto- and cross-correlation of logarithmic amplitude and phase can be

computed by

$$\begin{aligned} \langle u_1 u_2 \rangle'(d) &= \langle u_1 u_2 \rangle(d) / \langle u^2 \rangle, \\ \langle \phi_1 \phi_2 \rangle'(d) &= \langle \phi_1 \phi_2 \rangle(d) / \langle \phi^2 \rangle, \\ \langle u_1 \phi_2 \rangle'(d) &= \langle u_1 \phi_2 \rangle(d) / (\langle u^2 \rangle \langle \phi^2 \rangle)^{1/2}, \end{aligned} \quad (8)$$

where $\langle u^2 \rangle$ corresponds to $\langle u_1 u_2 \rangle(0)$ and $\langle \phi^2 \rangle$ to $\langle \phi_1 \phi_2 \rangle(0)$.

5.2. Numerical measurement and features

We analyze the auto- and cross-correlation of the logarithmic amplitude and phase from our numerical modelling. The wave function (Ψ_r) for a wave with

amplitude A_r and phase φ_r at a receiver is given by (Chernov, 1960)

$$\Psi_r = A_r e^{i\varphi_r}. \quad (9)$$

Wave propagation in random media incorporates a change in amplitude and phase, and the relative am-

plitude and phase changes can be written as

$$\ln \left(\frac{\Psi_r}{\Psi_0} \right) = \ln \left(\frac{A_r}{A_0} \right) + i(\varphi_r - \varphi_0), \quad (10)$$

where parameters with subscript 0 are the values for the incident waves (i.e., waves in homogeneous media). The log amplitude ratio ($\ln(A_r/A_0)$) corresponds to u_r in (7), and the phase difference ($\varphi_r - \varphi_0$) corresponds to ϕ_r .

In previous field-data studies (e.g., Aki, 1973), the log amplitude and phase fluctuation were analyzed by using the mean amplitude and traveltimes of plane waves arriving at a localized dense seismic array, with the assumption that the mean amplitude and traveltimes are equal to those of waves in the background homogeneous medium. However, in fact, waves lose their energy while propagating through random media due to scattering (e.g., Wu, 1982b), and the traveltimes tend to decrease due to the preference of waves for faster paths (Müller et al., 1992). In addition, the primary waves are contaminated by coherent scattered waves (Section 3). For scattering attenuation (Q_s^{-1}) of about 0.001 for weak perturbations with $\epsilon < 10\%$ (see Fig. 7), the amplitude change due to scattering attenuation is negligible in the estimation of amplitude fluctuation in the Earth. On the other hand, the traveltime anomalies play a major role in producing a biased result in the analysis of phase fluctuation; the median-line of the phase auto-correlation lies above zero. We perform fluctuation analyses using the mean amplitude and mean traveltime as reference levels for the calculation of the transmission fluctuations.

The transmission fluctuations for low-perturbation strengths ($\epsilon < 5\%$) agree with the theoretical expectation that the transmission fluctuation is determined consistently regardless of the perturbation level. However, the discrepancies start to increase for high-perturbation levels, $\epsilon = 8.5\%$, 10% (Fig. 9). The cross-correlation values at $r = 0$ increase with perturbation strength since both the fluctuation level and the traveltime anomaly increase with the strength of perturbation.

The spatial correlation of the transmission fluctuation is similar between different types of media (Fig. 10). However, the similarity does not hold when the distribution of heterogeneities is changed. Fig. 11 shows

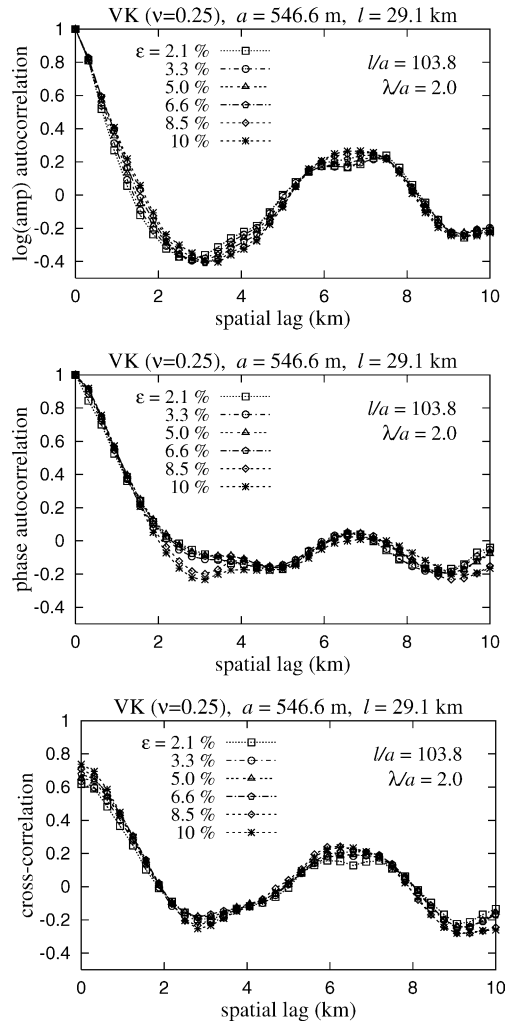


Fig. 9. Transmission fluctuations for amplitude and phase in random media (von Karman, $\nu = 0.25$, $a = 546.6$ m, $l = 29.1$ km) for various perturbation strengths ($\epsilon = 2.1\%$, 3.3% , 5.0% , 6.5% , 8.5% , 10%). The transmission fluctuation is nearly independent of the change in perturbation strength. Some obvious differences are observed in the phase autocorrelation.

the transmission fluctuations of 20 different realizations of the same medium, with the same parameters (e.g., ACF, a , ϵ), at various propagation distances ($l = 2.42$ – 29.1 km). The consistency between the curves reduces with an increase in the spatial lag, and each curve displays an individual variation at large spatial lag. As discussed in Section 3, the phases of scattered waves are dependent on the propagation path, and a differ-

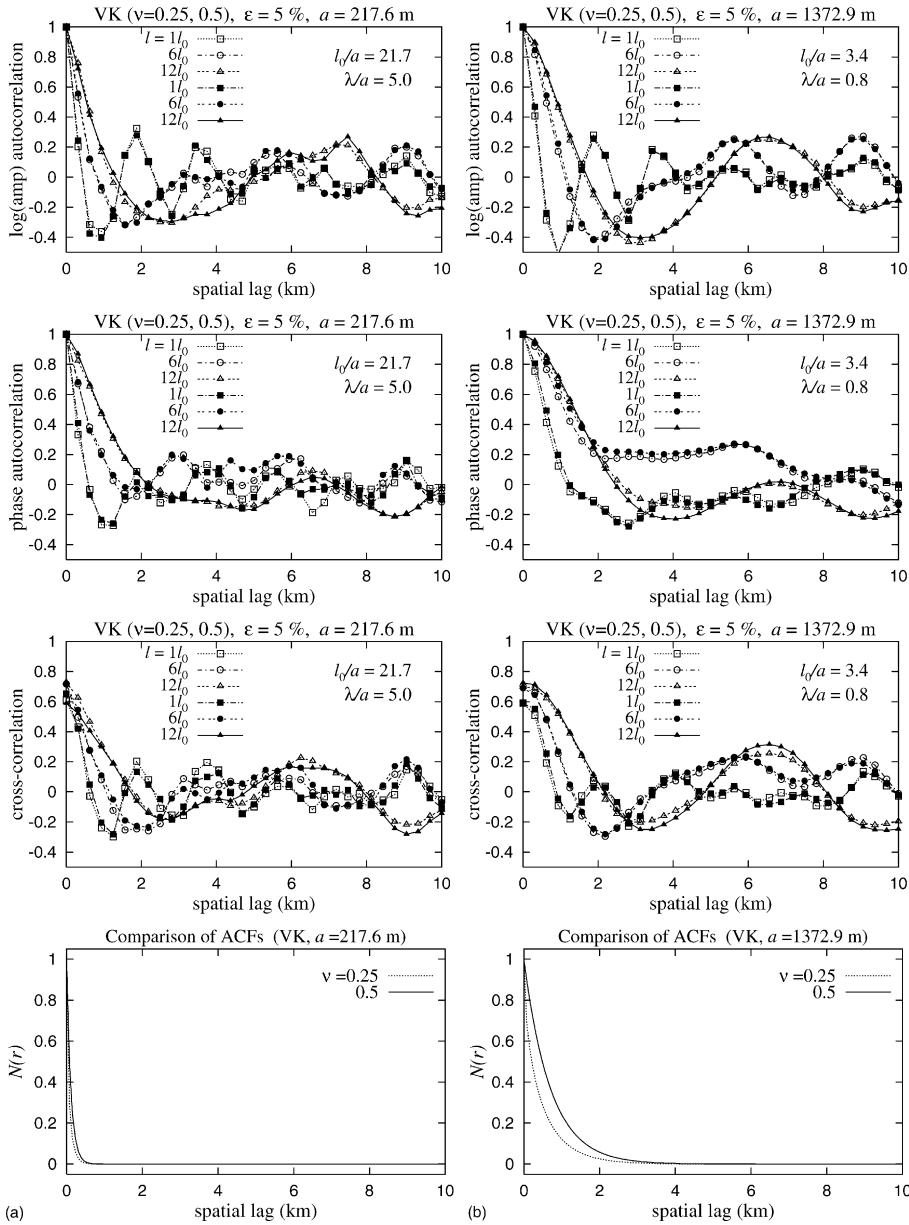


Fig. 10. Comparisons of transmission fluctuations between two different von Karman models ($\nu = 0.25, 0.5$) with a perturbation strength of 5% at various propagation distances ($l = 1l_0, 6l_0, 12l_0$, where $l_0 = 2.42$ km). The correlation lengths (a) for the heterogeneity are (a) 217.9 m and (b) 1372.9 m. The variation of auto-correlation functions (ACFs) with spatial lag is presented in the bottom of panel. Here, the von Karman medium with $\nu = 0.5$ corresponds to the exponential media. Slight changes in the transmission fluctuation are observed. However, in general, it is hard to distinguish the type of medium from the variation pattern even though there is a distinct difference between the two ACFs (e.g., at $a = 1372.9$ m).

ent combination of heterogeneities generates a different fluctuation pattern. The distinct fluctuations of the different model realizations do not decrease with propagation distance (compare the figures for $l = 1l_0$ and $12l_0$), but the deviation from the ensemble-averaged values (the filled circles in the figure) of the curves is rather consistent.

The overall trends of log amplitude auto-correlation and the cross-correlation of amplitude and phase appear

to be close to the theoretical variation of (8). Here, note that we consider a normalized cross-covariance of log amplitude and phase $(\langle u_1 \phi_2 \rangle(d) / \langle u_1 \phi_2 \rangle(0))$ in Fig. 11 so that we can observe its characteristic variation without the modulation by the variance of auto-correlations of log amplitude and phases. The comparison between the ensemble-averaged phase auto-correlation and theoretical variation, however, displays a discrepancy in the dependency on the spatial lag. This

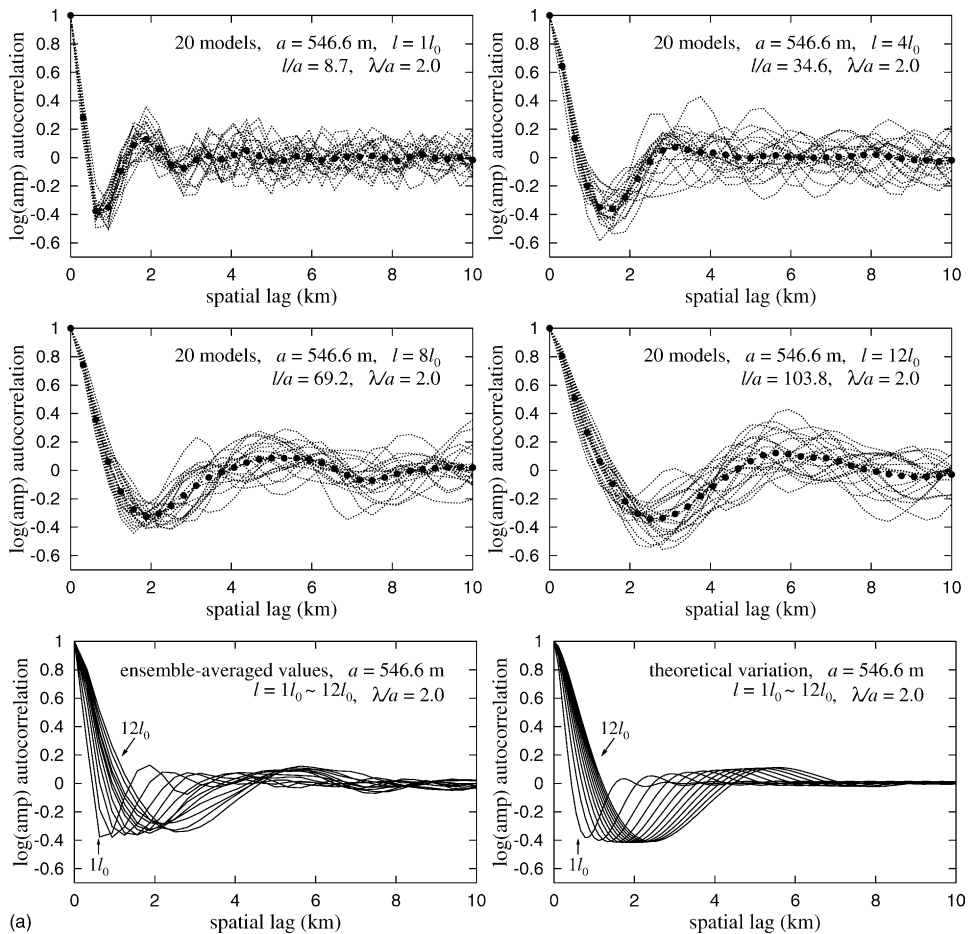


Fig. 11. Transmission fluctuations of 20 differently model realizations at various propagation distances ($l = 1l_0$ – $12l_0$). The random media are represented using an exponential ACF with $a = 546.6$ m and $\epsilon = 5\%$. The background wavespeed is 2.5 km/s and the dominant frequency of incident waves is 4.5 Hz. Filled circles represent the mean variation (ensemble-average) of 20 results with different realizations of the construction of random models: (a) auto-correlation of logarithmic amplitude, (b) auto-correlation of phase, and (c) normalized cross-covariance of log amplitude and phase. The ensemble-averaged variations (the left and bottom panels) of the log amplitude auto-correlation and the cross-correlation are very close to the theoretical prediction (the right and bottom panels), but the phase auto-correlation displays a different dependence on spatial lag.

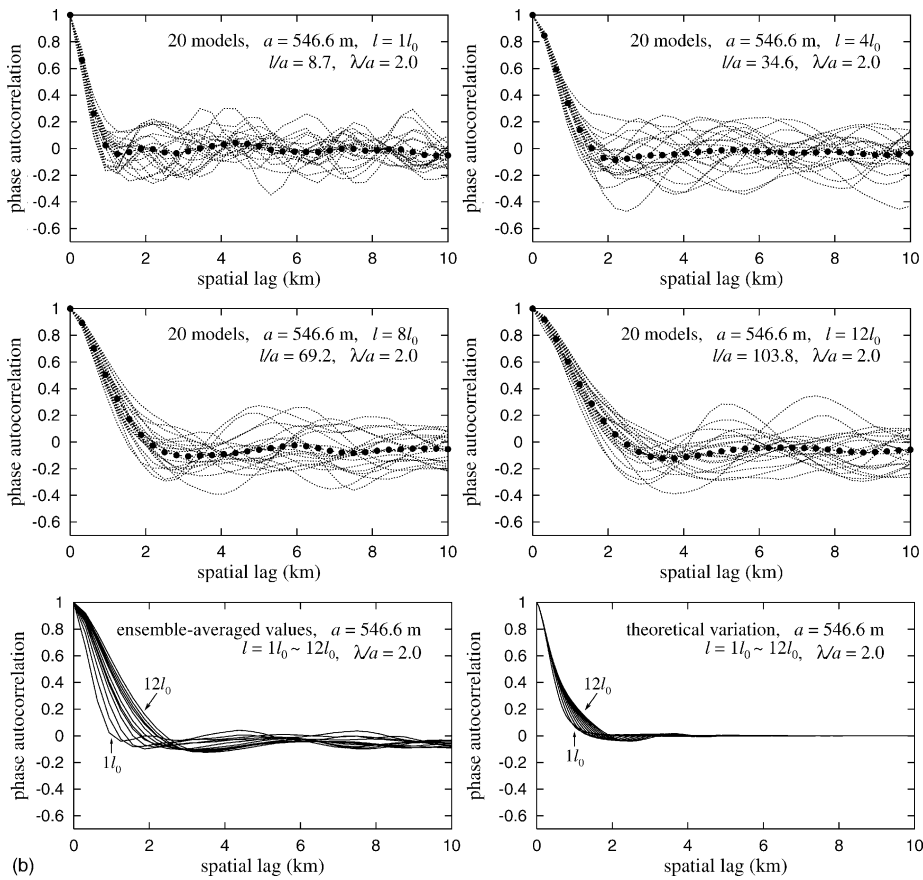


Fig. 11. (Continued)

difference seems to result from the fundamental assumption that the mean traveltimes will be equal to the traveltimes of waves in the homogeneous background medium. However, each time response for a random heterogeneous medium is contaminated by both the traveltimes shift and coherent scattered waves, which increase with perturbation strength. Thus, the theoretical prediction based on weak scattering approximation does not appear to be suitable for the estimation of phase fluctuation.

For geophysical inversion for the physical parameters of random heterogeneities in the Earth, the comparison of field results for amplitude and phase fluctuation with the theoretical variations can be unsta-

ble. Similar discrepancies between numerical results and theoretical estimates was found in [Line et al. \(1998\)](#). From our numerical experiments, the amplitude fluctuation can be predicted more accurately by the theory than phase fluctuation. The ensemble average of the transmission fluctuation of amplitude and phase, however, can provide stable results. Thus, the combination of results from various events with different propagation trajectories, recorded at the same receiver array, allows the extraction of ensemble-averaged values from which inferences can be made for the physical parameters of the medium. More theoretical studies are needed for a better prediction of phase fluctuation.

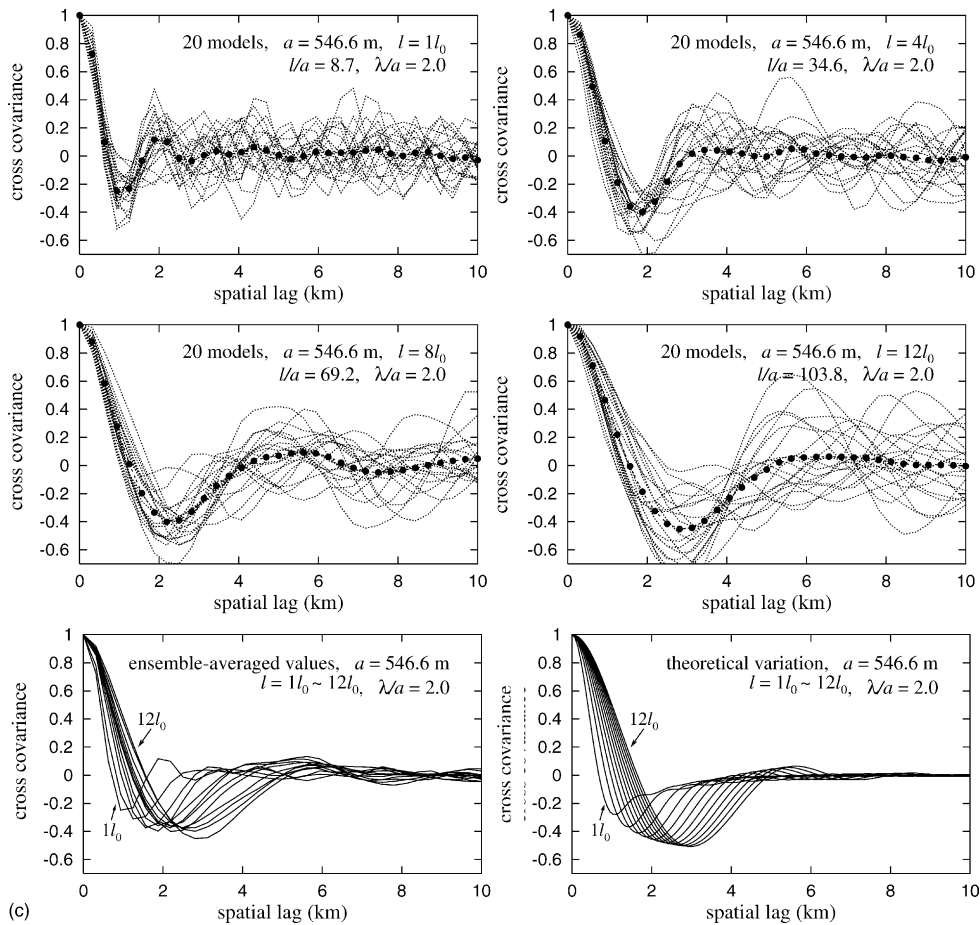


Fig. 11. (Continued).

6. Discussion and conclusions

Scattered waves in random media reveal various imprints of stochastic variations such as the generation of coherent scattered waves, a frequency shift in the dominant frequency, dependence of the normalized scattering attenuation on the perturbation level, and fluctuations of amplitude and phase in transmission depending on the propagation distance.

For stable measurement of the scattering attenuation, the time responses recorded at a sufficiently large distance are needed. An empirical condition is suggested as a function of dimensionless propagation distance terms, which incorporate propagation distance and correlation length with the wavelength. The mag-

nitude of the coherent scattered waves is proportional to the correlation length of heterogeneities in media. Thus, the normalized scattering attenuation (Q_s^{-1}/ϵ^2) decreases with the perturbation strength (ϵ) in the large wavenumber regime ($ka > 1$), while it is nearly constant regardless of the change of perturbation strength at low ka ($ka < 1$).

The fluctuations of amplitude and phase in transmission are dependent on propagation path, and different fluctuation patterns are observed for differently realizations of a stochastic medium. The ensemble-averaged amplitude fluctuation of 20 differently realized models is very close to the predicted theoretical variation, while the ensemble-averaged phase fluctuation displays a different form of variation with spatial lag than the theo-

retical results. The difference appears to be associated with the influence of the stochastic medium on the mean traveltimes through both coherent scattered waves and the preference of waves for faster paths.

Each transmission fluctuation for a differently realized random model exhibits a distinct variation at a large spatial lag. This indicates that the transmission fluctuations are a stochastic result of interference with heterogeneities close to propagation paths. The amplitude of the variation hardly decreases with propagation distance. Thus, the self-averaging process of the wavefield during propagation over a long distance does not look to be equivalent to the ensemble-averaging process of stacking the results from differently realized models.

The transmission fluctuation analysis is applicable to regional and far-field seismic field data (Aki, 1973; Capon, 1974; Flatté and Wu, 1988). However, in such application, the representation of media in terms of stochastic random media may not provide sufficient resolution of localized discrete heterogeneities (e.g., Vidale and Earle, 2000). The ensemble average of transmission fluctuation looks to be useful for the investigation of the mean perturbation in a given area. In particular, the ensemble-average technique is promising for the investigation of fine-scale heterogeneities. For this purpose, various events with different propagation trajectories can be combined to produce ensemble-averaged results.

Acknowledgements

We thank an anonymous reviewer for constructive review comments. We acknowledge the Australian National University Supercomputer Facility for allocation of computational time on the Alpha server.

References

- Aki, K., 1973. Scattering of P waves under the Montana Lasa. *J. Geophys. Res.* 78, 1334–1346.
- Aki, K., Chouet, B., 1975. Origin of coda waves: source, attenuation, and scattering effects. *J. Geophys. Res.* 80, 3322–3342.
- Aki, K., Richards, P.G., 1980. *Quantitative Seismology, Theory and Methods*, Vol. 1. W.H. Freeman and Company, San Francisco.
- Capon, J., 1974. Characterization of crust and upper mantle structure under LASA as a random medium. *Bull. Seism. Soc. Am.* 64, 235–266.
- Chernov, L.A., 1960. *Wave Propagation in a Random Medium*. McGraw-Hill, New York.
- Del Pezzo, E., Ibañez, J., Morales, J., Akinci, A., Maresca, R., 1995. Measurements of intrinsic and scattering seismic attenuation in the crust. *Bull. Seism. Soc. Am.* 85, 1373–1380.
- Flatté, S.M., Dashen, R., Munk, W.H., Watson, K.M., Zahariassen, F., 1979. *Sound Transmission Through a Fluctuating Ocean*. Cambridge University Press, New York.
- Flatté, S.M., Wu, R.-S., 1988. Small-scale structure in the lithosphere and asthenosphere deduced from arrival time and amplitude fluctuations at NORSAR. *J. Geophys. Res.* 93, 6601–6614.
- Frankel, A., Clayton, R.W., 1986. Finite difference simulations of seismic scattering: implications for the propagation of short-period seismic waves in the crust and models of crustal heterogeneities. *J. Geophys. Res.* 91, 6465–6489.
- Frenje, L., Juhlin, C., 2000. Scattering attenuation: 2-D and 3-D finite difference simulations vs. theory. *J. Appl. Geophys.* 44, 33–46.
- Giampiccolo, E., Gresta, S., Rasconá, F., 2004. Intrinsic and scattering attenuation from observed seismic codas in Southeastern Sicily (Italy). *Phys. Earth Planet. Inter.* 145, 55–66.
- Hedlin, M.A.H., Shearer, P.M., Earle, P.S., 1997. Seismic evidence for small-scale heterogeneity throughout the Earth's mantle. *Nature* 387, 145–150.
- Hong, T.-K., 2004. Scattering attenuation ratios of P and S waves in elastic media. *Geophys. J. Int.* 158, 211–224.
- Hong, T.-K., Kennett, B.L.N., 2002a. A wavelet-based method for simulation of two-dimensional elastic wave propagation. *Geophys. J. Int.* 150, 610–638.
- Hong, T.-K., Kennett, B.L.N., 2002b. On a wavelet-based method for the numerical simulation of wave propagation. *J. Comput. Phys.* 183, 577–622.
- Hong, T.-K., Kennett, B.L.N., 2003a. Scattering attenuation of 2-D elastic waves: theory and numerical modelling using a wavelet-based method. *Bull. Seism. Soc. Am.* 93, 922–938.
- Hong, T.-K., Kennett, B.L.N., 2003b. Modelling of seismic waves in heterogeneous media using a wavelet-based method: application to fault and subduction zones. *Geophys. J. Int.* 154, 483–498.
- Hong, T.-K., Kennett, B.L.N., 2004. Scattering of elastic waves in media with a random distribution of fluid-filled cavities: theory and numerical modelling. *Geophys. J. Int.*, in press.
- Hong, T.-K., Kennett, B.L.N., Wu, R.-S., 2004. Effects of the density perturbation in scattering. *Geophys. Res. Lett.* 31 (13), L13602, doi:10.1029/2004GL019933.
- Hoshihara, M., 2000. Large fluctuation of wave amplitude produced by small fluctuation of velocity structure. *Phys. Earth Planet. Inter.* 120, 201–217.
- Hoshihara, M., Rietbrock, A., Scherbaum, F., Nakahara, H., Haberland, C., 2001. Scattering attenuation and intrinsic absorption using uniform and depth dependent model- application to full seismogram envelope recorded in Northern Chile. *J. Seism.* 5, 157–179.
- Kaelin, B., Johnson, L.R., 1998a. Dynamic composite elastic medium theory. Part I. One-dimensional media. *J. Appl. Phys.* 84 (10), 5451–5457.
- Kaelin, B., Johnson, L.R., 1998b. Dynamic composite elastic medium theory. Part II. Three-dimensional media. *J. Appl. Phys.* 84 (10), 5458–5468.

- Kanasewich, E.R., 1981. *Time Sequence Analysis in Geophysics*, third ed. The University of Alberta Press, Alberta, Canada.
- Kawahara, J., 2002. Cutoff scattering angles for random acoustic media. *J. Geophys. Res.* 107 (B1) 10.1029/2001JB000429.
- Korn, M., 1993. Determination of site-dependent scattering Q from P-wave coda analysis with an energy-flux model. *Geophys. J. Int.* 113, 54–72.
- Line, C.E.R., Hobbs, R.W., Hudson, J.A., Synder, D.B., 1998. Statistical inversion of controlled-source seismic data using parabolic wave scattering theory. *Geophys. J. Int.* 132, 61–78.
- Müller, G., Roth, M., Korn, M., 1992. Seismic-wave traveltimes in random media. *Geophys. J. Int.* 110, 29–41.
- Müller, T.M., Shapiro, S.A., 2001. Most probable seismic pulses in single realizations of two- and three-dimensional random media. *Geophys. J. Int.* 144, 83–95.
- Nakahara, H., Sato, H., Ohtake, M., Nishimura, T., 1999. Spatial distribution of high-frequency energy radiation on the fault of the 1995 Hyogo-Ken Nanbu, Japan, earthquake (M_w 6.9) on the basis of the seismogram envelope inversion. *Bull. Seism. Soc. Am.* 89 (1), 22–35.
- Nishimura, T., Uchida, N., Sato, H., Ohtake, M., Tanaka, S., Hamaguchi, H., 2000. Temporal changes of the crustal structure associated with the M6.1 earthquake on September 3, 1998, and the volcanic activity of Mount Iwate, Japan. *Geophys. Res. Lett.* 27, 269–272.
- Nishimura, T., Yoshimoto, K., Ohtaki, T., Kanjo, K., Purwana, I., 2002. Spatial distribution of lateral heterogeneity in the upper mantle around the western Pacific region as inferred from analysis of transverse components of teleseismic P-coda. *Geophys. Res. Lett.* 29 (23), 2137, doi:10.1029/2002GL015606.
- Ratdomopurbo, A., Poupinet, G., 1995. Monitoring a temporal change of seismic velocity in a volcano: application to the 1992 eruption of Mt. Merapi (Indonesia). *Geophys. Res. Lett.* 22, 775–778.
- Roth, M., Korn, M., 1993. Single scattering theory versus numerical modelling in 2-D random media. *Geophys. J. Int.* 112, 124–140.
- Sato, H., 1982. Amplitude attenuation of impulsive waves in random media based on travel time corrected mean wave formalism. *J. Acoust. Soc. Am.* 71, 559–564.
- Sato, H., 1989. Broadening of seismogram envelopes in the randomly inhomogeneous lithosphere based on the parabolic approximation: southeastern Honshu, Japan. *J. Geophys. Res.* 94 (B12), 17,735–17,747.
- Sato, H., Fehler, M., 1998. *Seismic Wave Propagation and Scattering in the Heterogeneous Earth*. Springer-Verlag, New York.
- Shapiro, S.A., Kneib, G., 1993. Seismic attenuation by scattering: theory and numerical results. *Geophys. J. Int.* 114, 373–391.
- Shapiro, S.A., Schwarz, R., Gold, N., 1996. The effect of random isotropic inhomogeneities on the phase velocity of seismic waves. *Geophys. J. Int.* 127, 783–794.
- Singh, S.K., Pacheco, J., Ordaz, M., Kostoglodov, V., 2000. Source time function and duration of Mexican earthquakes. *Bull. Seism. Soc. Am.* 90, 468–482.
- Sivaji, C., Nishizawa, O., Kitagawa, G., Fukushima, Y., 2002. A physical-model study of the statistics of seismic waveform fluctuations in random heterogeneous media. *Geophys. J. Int.* 148, 575–595.
- Snieder, R., Alexandre, G., Douma, H., Scales, J., 2002. Coda wave interferometry for estimating nonlinear behavior in seismic velocity. *Science* 295, 2253–2255.
- Tselentis, G.-A., 1998. Intrinsic and scattering seismic attenuation in W. Greece. *Pure Appl. Geophys.* 153, 703–712.
- Ugalde, A., Pujades, L.G., Canas, J.A., Villaseñor, A., 1998. Estimation of the intrinsic absorption and scattering attenuation in Northeastern Venezuela (Southeastern Caribbean) using coda waves. *Pure Appl. Geophys.* 153, 685–702.
- Vidale, J.E., Earle, P., 2000. Fine-scale heterogeneity in the Earth's inner core. *Nature* 404, 273–275.
- Wennerberg, L., 1993. Multiple scattering interpretations of coda Q measurements. *Bull. Seism. Soc. Am.* 83, 279–290.
- Wu, R.-S., 1982a. Mean field attenuation and amplitude attenuation due to wave scattering. *Wave Motion* 4, 305–316.
- Wu, R.-S., 1982b. Attenuation of short period seismic waves due to scattering. *Geophys. Res. Lett.* 9, 9–12.
- Wu, R.-S., Aki, K., 1988. Introduction: seismic wave scattering in three-dimensionally heterogeneous Earth. *Pure Appl. Geophys.* 128, 1–6.
- Wu, R.-S., Flatté, S.M., 1990. Transmission fluctuations across an array and heterogeneities in the crust and upper mantle. *Pure Appl. Geophys.* 132, 175–196.
- Yoshimoto, K., Sato, H., Ito, Y., Ohminata, T., Ohtake, M., 2002. Frequency-dependent attenuation of high-frequency P and S waves in the upper crust in Western Nagano, Japan. *Pure Appl. Geophys.* 153, 489–502.